

Light-Induced Type-II Band Inversion and Quantum Anomalous Hall State in Monolayer FeSe

Z. F. Wang,^{1,*} Zhao Liu,¹ Jinlong Yang,² and Feng Liu^{3,4,†}

¹Hefei National Laboratory for Physical Sciences at the Microscale,
CAS Key Laboratory of Strongly-Coupled Quantum Matter Physics,
University of Science and Technology of China, Hefei, Anhui 230026, China

²Hefei National Laboratory for Physical Sciences at the Microscale,
Synergetic Innovation Center of Quantum Information and Quantum Physics,
University of Science and Technology of China, Hefei, Anhui 230026, China

³Department of Materials Science and Engineering, University of Utah, Salt Lake City, Utah 84112, USA

⁴Collaborative Innovation Center of Quantum Matter, Beijing 100084, China



(Received 19 December 2017; published 13 April 2018)

Coupling a quantum anomalous Hall (QAH) state with a superconducting state offers an attractive approach to detect the signature alluding to a topological superconducting state [Q. L. He *et al.*, *Science* **357**, 294 (2017)], but its explanation could be clouded by disorder effects in magnetic doped QAH materials. On the other hand, an antiferromagnetic (AFM) quantum spin Hall (QSH) state is identified in the well-known high-temperature 2D superconductor of monolayer FeSe [Z. F. Wang *et al.*, *Nat. Mater.* **15**, 968 (2016)]. Here, we report a light-induced type-II band inversion (BI) and a QSH-to-QAH phase transition in the monolayer FeSe. Depending on the handedness of light, a spin-tunable QAH state with a high Chern number of ± 2 is realized. In contrast to the conventional type-I BI resulting from intrinsic spin-orbital coupling (SOC), which inverts the band an odd number of times and respects time reversal symmetry, the type-II BI results from a light-induced handedness-dependent effective SOC, which inverts the band an even number of times and does not respect time reversal symmetry. The interplay between these two SOC terms makes the spin-up and -down bands of an AFM QSH state respond oppositely to a circularly polarized light, leading to the type-II BI and an exotic topological phase transition. Our finding affords an exciting opportunity to detect Majorana fermions in one single material without magnetic doping.

DOI: [10.1103/PhysRevLett.120.156406](https://doi.org/10.1103/PhysRevLett.120.156406)

A recent experiment has reported an interesting “smoking gun” of a transport signature to detect Majorana fermions in a combined superconductor and quantum anomalous Hall (QAH) system [1]. Later on, however, it was argued that the observed signature can also be explained by disorder effects [2,3]. Since disorder is unavoidable in magnetic doped QAH materials, it will be highly desirable to combine a superconducting and QAH state without magnetic doping to eliminate disorder effects. In this Letter, we will demonstrate that this intriguing scenario can be realized in the high-temperature 2D superconductor of monolayer FeSe, through an exotic light-induced quantum spin Hall (QSH)-to-QAH topological phase transition.

There has been great research interest to search and design novel topological materials as well as to manipulate topological phase transitions. As two closely linked topological phases, the QSH [4–7] and QAH [8–11] states have been extensively studied in the past decade. In general, QSH states exist in nonmagnetic materials, and QAH states in ferromagnetic materials [11]; a QSH state can be tuned into a QAH state by including an exchange field through magnetic doping [9,10]. An exception is the antiferromagnetic (AFM)

topological states [12–20], which are magnetic but without net magnetization. The combined topological and AFM spin order provides intriguing opportunities to study exotic quantum phenomena.

On the other hand, the high-temperature 2D superconductor of FeSe has inspired great experimental [21–25] and theoretical [26–29] interests. Often times the parent material of a superconductor has an AFM spin order, and possible topological states in FeSe are expected [30–34]. Very interestingly, an AFM QSH state has been recently theoretically predicted and experimentally identified in monolayer FeSe [35]. Here, starting from this AFM QSH state, we further demonstrate a spin-tunable QAH state induced by circularly polarized light irradiation, based on first-principles tight-binding calculations.

We show that with increasing light intensity, the left- or right-handed circularly polarized light will induce a monotonic increase of the band gap for a spin-up or -down band around the M point, but a band inversion (BI) for a spin-down or -up band characterized with a sign change of its Chern number, which we call it a type-II BI. This in turn leads to the formation of a QAH state with a high Chern

number of either -2 or 2 , as identified by calculations of both edge states and the quantized conductivity. An effective $k \cdot p$ Hamiltonian is derived and an analytic expression for the light-induced effective spin-orbital coupling (ESOC) is obtained. The ESOC is handedness dependent, in contrast to the intrinsic spin-orbital coupling (SOC), which is spin dependent. The interplay between the two contrasting SOC terms causes an opposite response of spin-up and -down bands to the light, leading to the type-II BI and an exotic QSH-to-QAH phase transition.

We first illustrate the type-II BI in comparison with the conventional BI, which we call type-I, as shown in Fig. 1. The type-I BI has provided a fundamental understanding of the difference between a normal insulator (NI) and a QSH state. For example, starting from a narrow charge gap semiconductor, its valence and conduction band-edge state has an odd (even) and even (odd) parity, respectively. With increasing intrinsic SOC, the charge gap closes and then reopens a SOC gap with the parity of the band-edge states inverted, and hence the system becomes nontrivial for both spin components to realize a QSH state [Fig. 1(a)]. Generally, the type-I BI inverts the band an odd number of times (typically one time), which underlies almost all the topological transitions [5,36–38] known to date. In contrast, Fig. 1(b) illustrates the type-II BI that inverts the band an even number of times and underlies a QSH-to-QAH phase transition, in which both spin components remain nontrivial after BI. It is induced by a light-induced ESOC instead of an intrinsic SOC. Starting from a QSH state with an SOC gap [Fig. 1(b)], with increasing ESOC, the SOC gap of one spin component (let us say spin down) decreases while that of the spin-up component increases. Then, the spin-down gap closes and reopens with its band topology changing to an opposite sign of the Chern number (by a mod of 2), and hence the system is nontrivial for both spin components and becomes a high-Chern-number QAH state.

A QSH state can be considered as two copies of spin-up or -down QAH states. The SOC is spin dependent, reversing its action on opposite spins (respecting time reversal symmetry). Consequently, it closes and reopens the

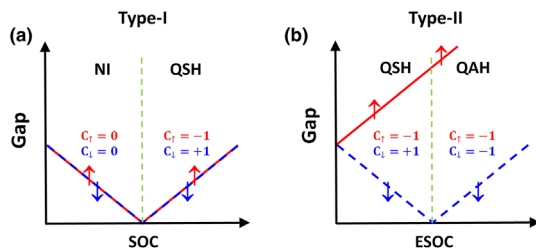


FIG. 1. (a) Type-I BI for a NI-to-QSH phase transition with increasing intrinsic SOC. (b) Type-II BI for a QSH-to-QAH phase transition with increasing light-induced ESOC. The red and blue colors denote spin-up (up arrow) and spin-down (down arrow) bands, respectively. The corresponding Chern numbers for the spin-up and spin-down bands are labeled before and after BI.

gap for both spin components simultaneously, resulting in the type-I BI [Fig. 1(a)]. The ESOC is handedness dependent, having the opposite action on opposite spins (breaking the time reversal symmetry). Consequently, it closes and reopens the gap of one spin component while increasing continuously the gap of the other spin component, resulting in the type-II BI [Fig. 1(b)].

After illustrating the concept of type-II BI, next we demonstrate its realization in monolayer FeSe. The band structure of monolayer FeSe in checkerboard AFM spin order with SOC is shown in Fig. 2(a). One can see an indirect SOC gap around the M point (see also Fig. S1) [39], which supports an AFM QSH state as identified previously [35]. This band structure is drastically modified, as shown in Figs. 2(b)–2(e), under a time-dependent irradiation of light $\vec{A} = A[\eta \sin(\omega\tau)\hat{x} + \cos(\omega\tau)\hat{y}]$, where ω is the frequency, A is the amplitude of the vector potential, and $\eta = \pm 1$ denotes the handedness of the right- or left-handed circularly polarized light. The band structures under light irradiation are calculated using the Floquet theory with a first-principles tight-binding Hamiltonian [39,40]. With increasing light intensity, the spin degeneracy is lifted as the spin-up and -down bands have an opposite response to the light around the M point. The gap (E_g^1) of the spin-down band (blue color) first closes and then reopens, while the gap (E_g^2) of the spin-up band (red color) increases monotonically, as shown in Fig. 2(f).

Generally, the process of band gap closing and reopening indicates a BI accompanied with a topological phase transition [5,36–38]. In order to identify the new phase caused by BI, the band structure of a ferromagnetic-edged FeSe ribbon with a width of 30 unit cells is calculated. For comparison, we first show the ribbon band before BI at a relatively low light intensity ($eA/\hbar = 0.2 \text{ \AA}^{-1}$). The spin- z component, and the left- and right-edge projected band structures are shown in Figs. 3(a), 3(b), and 3(c), respectively. Within the gap, one sees that each edge has two edge states with opposite propagating direction and opposite spin- z orientation. Each pair of edge states forms an asymmetric Dirac cone, which is consistent with the results without light irradiation [35]. Comparing the two edges, one notices that the edge states with the same spin- z orientation propagate in opposite directions along the left and right edge, respectively. These are characteristic features of topological edge states, indicating that the light irradiated FeSe remains in the QSH state before BI, as schematically shown in Fig. 3(d).

Next, after BI at a sufficiently high light intensity ($eA/\hbar = 0.3 \text{ \AA}^{-1}$), the spin- z component and the left- and right-edge projected band structures are shown in Figs. 3(e), 3(f), and 3(g), respectively. A drastic change of the edge states is observed. Now each edge has two edge states with the same propagating direction but opposite spin- z orientation. The same-spin edge states propagate in opposite directions at the left and right edges, respectively. These features signify a

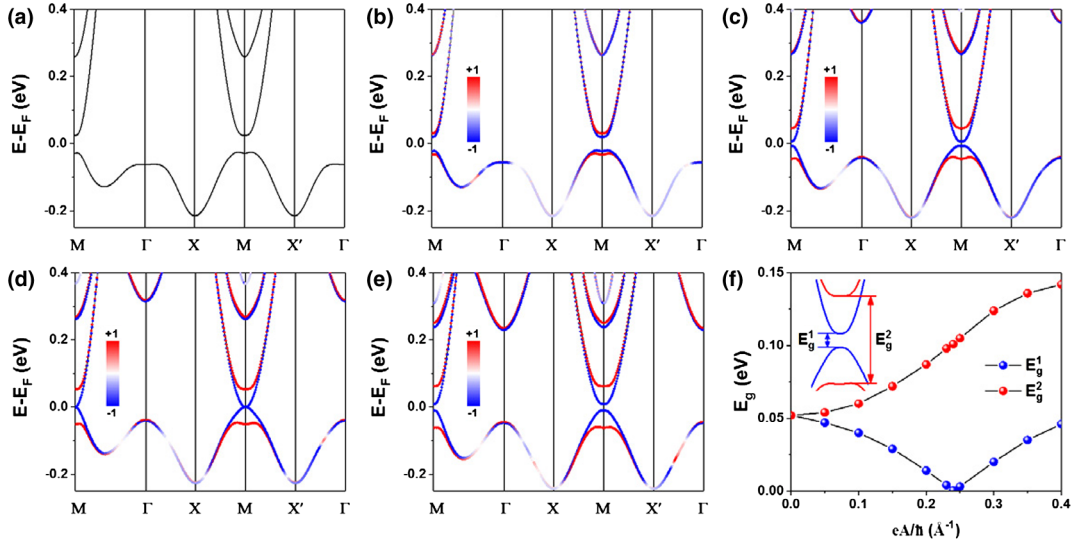


FIG. 2. (a)–(e) Band structure evolution of FeSe under the irradiation of left-handed circularly polarized light with a light intensity eA/\hbar of 0, 0.1, 0.2, 0.24, and 0.3 \AA^{-1} , respectively. The red and blue colors in (b)–(e) denote the up and down spin- z component, respectively. (f) The band gap evolution under the light irradiation. The inset is the enlarged band gap around the M point in (e) and the definition of E_g^1 and E_g^2 . In our calculations, the light energy $\hbar\omega$ is set to 8 eV, which is chosen to be larger than the band width of FeSe, so that the Floquet bands do not cross each other.

QAH state in the light irradiated FeSe after BI, as schematically shown in Fig. 3(h). We have also checked the spin- x and $-y$ component, which are negligible compared to the spin- z component. This guarantees the spin-momentum locking relation in both QSH and QAH edge states [41]. We note that only the spin-down band (blue color) is inverted by the left-handed circularly polarized light, so that the spin-down edge state reverses the propagating direction at both edges [blue arrows in Figs. 3(d) and 3(h)], resulting in a QSH-to-QAH

topological phase transition. Conversely, another QAH state can be obtained by using the right-handed circularly polarized light, in which the spin-up band will instead be inverted.

Beside edge states, an alternative way to distinguish the QSH from the QAH state is by spin Hall (σ_{xy}^s) and Hall (σ_{xy}) conductivity [42–44]. Figure 4 shows the calculated conductivity for both the left- and right-handed circularly polarized light. Before BI, a quantized spin Hall conductivity of $-2e/4\pi$ is obtained within the energy window of

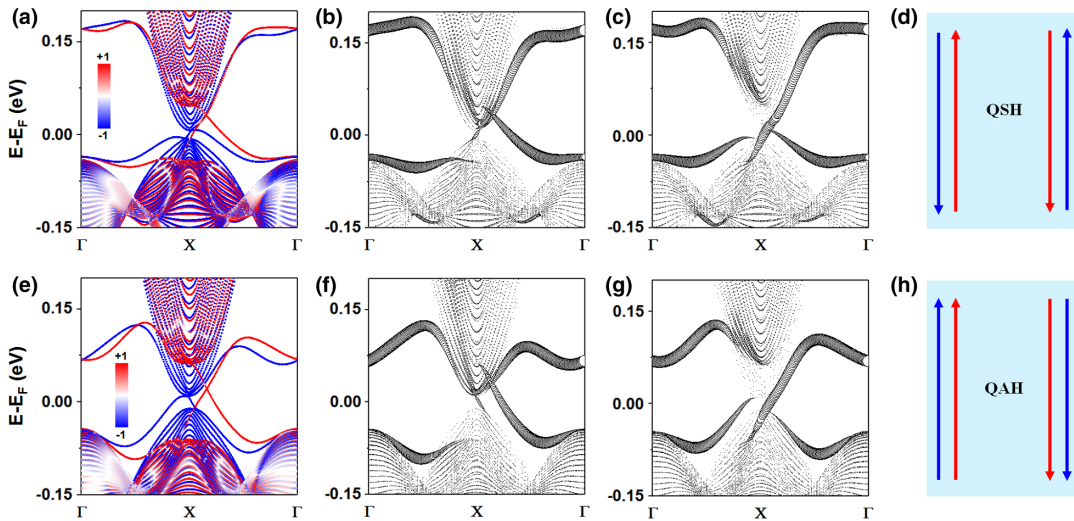


FIG. 3. (a)–(c),(e)–(g) Projected band structure of a FeSe ribbon with a ferromagnetic edge under the irradiation of left-handed circularly polarized light before and after BI with a light intensity eA/\hbar of 0.2 and 0.3 \AA^{-1} , respectively. (a),(e) Spin- z component projection. (b),(f) Left edge projection. (c),(g) Right edge projection. The red and blue colors denote the up and down spin- z component, respectively. The circle size denotes the weighting factor of the edge states. (d),(f) Schematic plot of the topological edge states for the QSH and QAH state shown in (a)–(c) and (e)–(g), respectively.

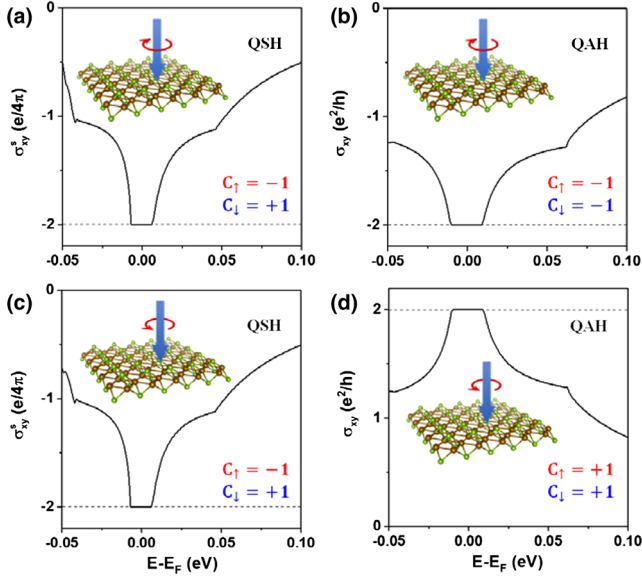


FIG. 4. (a),(b) Spin Hall and Hall conductivity under the irradiation of left-handed circularly polarized light before and after BI with a light intensity eA/\hbar of 0.2 and 0.3 \AA^{-1} , respectively. (c) and (d) are the same as (a) and (b), respectively, but under the irradiation of right-handed circularly polarized light. The insets show the handedness of the light, and the Chern number for the spin-up and -down band.

the band gap for both handednesses of light, as shown in Figs. 4(a) and 4(c). Thus, the spin Chern number $C_s = -1$ for this QSH state. The corresponding Chern number for the spin-up and -down band is $C_\uparrow = -1$ and $C_\downarrow = +1$, as labeled in the inset of Figs. 4(a) and 4(c), respectively. In contrast, after BI, the spin Hall conductivity is quenched to zero within the band gap, while a quantized Hall conductivity of $-2e^2/h$ and $2e^2/h$ is obtained for the left- and right-handed circularly polarized light, respectively, as shown in Figs. 4(b) and 4(d). Thus, the Chern number $C = -2$ and 2 for the QAH state under the left- and right-handed circularly polarized light, respectively. The spin-up and -down band have the Chern number of $C_\uparrow = C_\downarrow = -1$ and $+1$, as labeled in the inset of Figs. 4(b) and 4(d), respectively. From the analysis of the spin component in Figs. 2 and 3, we learned that the left- and right-handed circularly polarized light will induce a type-II BI for only the spin-down and -up band, respectively. Consequently, the sign of the Chern number is changed only for the inverted spin band but remains the same for the other spin band, hence realizing a QSH-to-QAH topological phase transition.

For the type-II BI shown above, the most significant feature is that the Chern number for the inverted spin band changes its sign only, but never quenches its value to zero. This behavior is rather unusual, indicating that the system is nontrivial both before and after BI. It is distinctively different from the type-I BI known previously [5,36–38] that underlies a phase transition between the trivial and

nontrivial state. For the type-I BI, the Chern number changes an odd number of times (typically 1). For example, magnetic doping [45] has been shown to also induce a QSH-to-QAH phase transition in HgTe, but with a Hall conductivity of $\pm e^2/h$ instead of $\pm 2e^2/h$ that we found here. It is because in HgTe one of the spin bands changes from nontrivial to trivial with its band inverted one time [45]. Here, the spin-up and -down bands are both nontrivial before and after BI, and one of the spin bands is inverted two times as reflected by the Chern number changing from $+1$ (-1) to -1 ($+1$).

To better understand this intriguing type-II BI, we present below a theoretical analysis based on an effective $k \cdot p$ Hamiltonian. Near the Fermi level, the band structure of FeSe around the M point is dominated by d_{xz} and d_{yz} orbitals, as shown in Fig. S2 [39]. Since the spin-up and -down bands are degenerate from our first-principles calculations and the on-site SOC term between the d_{xz} and d_{yz} orbitals is spin decoupled, one can decouple the spin-up and -down bands into two sublattices [27], as shown in Fig. S3 [39]. In each sublattice, one considers only one spin band with two orbitals of d_{xz} and d_{yz} per unit cell. Including both the nearest-neighbor and second nearest-neighbor hopping parameters and expanding around the M point, an effective $k \cdot p$ Hamiltonian can be obtained as [39]

$$H = a_0(k_x^2 + k_y^2)\sigma_0 + a_1k_xk_y\sigma_1 + a_2(k_x^2 - k_y^2)\sigma_3 + \lambda s\sigma_2, \quad (1)$$

where σ is the Pauli matrix, $s = \pm 1$ for spin up and down, and λ is the intrinsic SOC. As shown in Fig. S4 [39], without and with SOC the $k \cdot p$ bands are overlaid with the first-principles bands along high symmetry directions $X-M-X$ and $\Gamma-M-\Gamma$, and around the M point in the 2D BZ for both the valence band and conduction band. Very good agreement is seen not only along high symmetry directions but also around the M point, using the fitting parameters $a_0 = 0.75 \text{ eV \AA}^2$, $a_1 = 4.5 \text{ eV \AA}^2$, $a_2 = 1.25 \text{ eV \AA}^2$, and $\lambda = -0.0265 \text{ eV}$. Also the spin Berry curvature shows very good agreement between $k \cdot p$ and first-principles results (see Fig. S5) [39].

Then, based on Floquet theory [46–50], the photon-dressed effective Hamiltonian for FeSe under irradiation of a circularly polarized light can be written as [39]

$$H_F = a_0(k_x^2 + k_y^2)\sigma_0 + a_1k_xk_y\sigma_1 + a_2(k_x^2 - k_y^2)\sigma_3 + (\lambda s + \lambda'\eta)\sigma_2, \quad (2)$$

$$\lambda' = \frac{2}{\hbar\omega} \left(\frac{eA}{\hbar} \right)^2 (k_x^2 + k_y^2)a_1a_2 + \frac{1}{4\hbar\omega} \left(\frac{eA}{\hbar} \right)^4 a_1a_2.$$

Comparing Eqs. (1) and (2), one sees that an extra light-induced ESOC term ($\lambda'\eta$) is introduced, and its sign depends on handedness but not on spin. This new term is clearly different from the intrinsic SOC term (λs) and also

different from the conventional Zeeman term. Since $\lambda < 0$ and $\lambda' > 0$, the overall value of SOC ($\lambda s + \lambda' \eta$) will decrease (increase) if s and η have the same (different) sign. The critical point is defined by $\lambda s + \lambda' \eta = 0$ at the M point with $k = 0$, where the overall SOC vanishes and band gap closes. Consequently, the spin-up and -down bands will have an opposite response to the circularly polarized light of opposite handedness. For example, with increasing left-handed circularly polarized light intensity, the evolution of $k \cdot p$ band structure around the M point is shown in Fig. S6 [39], which shows a band gap closing and reopening process for the spin-down band, but a continuous increase of the band gap for the spin-up band. This is consistent with the results shown in Fig. 2.

From the photon-dressed effective Hamiltonian, the Chern number for the spin-up and -down band can be calculated as [39]

$$C_{\uparrow/\downarrow} = \begin{cases} +1, & (\lambda s + \lambda' \eta)_{k=0} > 0, \\ -1, & (\lambda s + \lambda' \eta)_{k=0} < 0. \end{cases} \quad (3)$$

Depending on the sign of $(\lambda s + \lambda' \eta)_{k=0}$, the Chern number for the spin-up and -down band can be either +1 or -1. This indicates that the interplay between ESOC and SOC determines the final value of the Chern number. We also point out that the gapless non-SOC band for FeSe with AFM spin order has played a significant role in giving rise to the observed type-II BI. Without any trivial mass term to open a trivial gap, the light-induced ESOC can completely cancel the intrinsic SOC and hence change its sign in the BI process. Consequently, no trivial phase will appear after type-II BI for the inverted band. This explains straightforwardly why our predicted QAH state has a different Hall conductivity compared to the HgTe system [45].

We thank Jiatao Sun for helpful discussions. This work is supported by NSFC (Grants No. 11774325 and No. 21603210), the National Key R&D Program of China (Grant No. 2017YFA0204904), the Chinese Youth One Thousand Talents Program, and the Fundamental Research Funds for the Central Universities. F.L. is supported by U.S. DOE-BES (Grant No. DE-FG02-04ER46148). We thank the Supercomputing Center at USTC for providing the computing resources.

* zfwang15@ustc.edu.cn

† fliu@eng.utah.edu

- [1] Q. L. He *et al.*, *Science* **357**, 294 (2017).
- [2] Y. Huang, F. Setiawan, and J. D. Sau, *Phys. Rev. B* **97**, 100501 (2018).
- [3] W. Ji and X.-G. Wen, *Phys. Rev. Lett.* **120**, 107002 (2018).
- [4] C. L. Kane and E. J. Mele, *Phys. Rev. Lett.* **95**, 226801 (2005).
- [5] B. A. Bernevig, T. L. Hughes, and S.-C. Zhang, *Science* **314**, 1757 (2006).

- [6] M. König, S. Wiedmann, C. Brune, A. Roth, H. Buhmann, L. W. Molenkamp, X.-L. Qi, and S.-C. Zhang, *Science* **318**, 766 (2007).
- [7] I. Knez, R.-R. Du, and G. Sullivan, *Phys. Rev. Lett.* **107**, 136603 (2011).
- [8] F. D. M. Haldane, *Phys. Rev. Lett.* **61**, 2015 (1988).
- [9] R. Yu, W. Zhang, H.-J. Zhang, S.-C. Zhang, X. Dai, and Z. Fang, *Science* **329**, 61 (2010).
- [10] C.-Z. Chang *et al.*, *Science* **340**, 167 (2013).
- [11] Y. Ren, Z. Qiao, and Q. Niu, *Rep. Prog. Phys.* **79**, 066501 (2016).
- [12] R. S. K. Mong, A. M. Essin, and J. E. Moore, *Phys. Rev. B* **81**, 245209 (2010).
- [13] C. Fang, M. J. Gilbert, and B. A. Bernevig, *Phys. Rev. B* **88**, 085406 (2013).
- [14] R. A. Muller, N. R. Lee-Hone, L. Lapointe, D. H. Ryan, T. Pereg-Barnea, A. D. Bianchi, Y. Mozharivskyj, and R. Flacau, *Phys. Rev. B* **90**, 041109 (2014).
- [15] J. Zhou, Q. F. Liang, H. Weng, Y. B. Chen, S. H. Yao, Y. F. Chen, J. Dong, and G. Y. Guo, *Phys. Rev. Lett.* **116**, 256601 (2016).
- [16] P. Zhou, C. Q. Sun, and L. Z. Sun, *Nano Lett.* **16**, 6325 (2016).
- [17] J. Liu, S. Y. Park, K. F. Garrity, and D. Vanderbilt, *Phys. Rev. Lett.* **117**, 257201 (2016).
- [18] X.-Y. Dong, S. Kanungo, B. Yan, and C.-X. Liu, *Phys. Rev. B* **94**, 245135 (2016).
- [19] J. Wang, *Phys. Rev. B* **95**, 115138 (2017).
- [20] N. Hao, F. Zheng, P. Zhang, and S.-Q. Shen, *Phys. Rev. B* **96**, 165102 (2017).
- [21] Q. Wang *et al.*, *Chin. Phys. Lett.* **29**, 037402 (2012).
- [22] S. He *et al.*, *Nat. Mater.* **12**, 605 (2013).
- [23] S. Tan *et al.*, *Nat. Mater.* **12**, 634 (2013).
- [24] J. J. Lee *et al.*, *Nature (London)* **515**, 245 (2014).
- [25] J.-F. Ge, Z.-L. Liu, C. Liu, C.-L. Gao, D. Qian, Q.-K. Xue, Y. Liu, and J.-F. Jia, *Nat. Mater.* **14**, 285 (2015).
- [26] K. Liu, Z.-Y. Lu, and T. Xiang, *Phys. Rev. B* **85**, 235123 (2012).
- [27] F. Zheng, Z. Wang, W. Kang, and P. Zhang, *Sci. Rep.* **3**, 2213 (2013).
- [28] S. Coh, M. L. Cohen, and S. G. Louie, *New J. Phys.* **17**, 073027 (2015).
- [29] H.-Y. Cao, S. Chen, H. Xiang, and X.-G. Gong, *Phys. Rev. B* **91**, 020504(R) (2015).
- [30] N. Hao and J. Hu, *Phys. Rev. X* **4**, 031053 (2014).
- [31] Z. Wang, P. Zhang, G. Xu, L. K. Zeng, H. Miao, X. Xu, T. Qian, H. Weng, P. Richard, A. V. Fedorov, H. Ding, X. Dai, and Z. Fang, *Phys. Rev. B* **92**, 115119 (2015).
- [32] G. Xu, B. Lian, P. Tang, X.-L. Qi, and S.-C. Zhang, *Phys. Rev. Lett.* **117**, 047001 (2016).
- [33] X. Wu, S. Qin, Y. Liang, H. Fan, and J. Hu, *Phys. Rev. B* **93**, 115129 (2016).
- [34] X. Shi, Z.-Q. Han, P. Richard, X.-X. Wu, X.-L. Peng, T. Qian, S.-C. Wang, J.-P. Hu, Y.-J. Sun, and H. Ding, *Science bulletin* **62**, 503 (2017).
- [35] Z. F. Wang *et al.*, *Nat. Mater.* **15**, 968 (2016).
- [36] M. Z. Hasan and C. L. Kane, *Rev. Mod. Phys.* **82**, 3045 (2010).
- [37] X.-L. Qi and S.-C. Zhang, *Rev. Mod. Phys.* **83**, 1057 (2011).

- [38] A. Bansil, Hsin Lin, and Tanmoy Das, *Rev. Mod. Phys.* **88**, 021004 (2016).
- [39] See Supplemental Material at <http://link.aps.org/supplemental/10.1103/PhysRevLett.120.156406> for details of calculation methods, additional first principles, and $k \cdot p$ results.
- [40] H. Liu, J. T. Sun, C. Cheng, F. Liu, and S. Meng, *arXiv*: 1710.05546.
- [41] B. Huang, K.-H. Jin, B. Cui, F. Zhai, J. Mei, and F. Liu, *Nat. Commun.* **8**, 15850 (2017).
- [42] Z. F. Wang, Z. Liu, and F. Liu, *Nat. Commun.* **4**, 1471 (2013).
- [43] Z. F. Wang, K.-H. Jin, and F. Liu, *Nat. Commun.* **7**, 12746 (2016).
- [44] Z. F. Wang, K.-H. Jin, and F. Liu, *Comput. Mol. Sci.* **7**, e1304 (2017).
- [45] C.-X. Liu, X.-L. Qi, X. Dai, Z. Fang, and S.-C. Zhang, *Phys. Rev. Lett.* **101**, 146802 (2008).
- [46] T. Kitagawa, T. Oka, A. Brataas, L. Fu, and E. Demler, *Phys. Rev. B* **84**, 235108 (2011).
- [47] N. H. Lindner, G. Refael, and V. Galitski, *Nat. Phys.* **7**, 490 (2011).
- [48] M. Ezawa, *Phys. Rev. Lett.* **110**, 026603 (2013).
- [49] H. Hübener¹, M. A. Sentef, U. D. Giovannini, A. F. Kemper, and A. Rubio, *Nat. Commun.* **8**, 13940 (2017).
- [50] M. S. Rudner, N. H. Lindner, E. Berg, and M. Levin, *Phys. Rev. X* **3**, 031005 (2013).